J Fluoresc (2007) 17:643–648
DOI 10.1007/s10895-006-0072-1

ORIGINAL PAPER

Quantitative Time-Resolved Fluorescence Spectrum of the Cortical Sarcoma and the Adjacent Normal Tissue

Yuezhi Li · Mingzhao Li · Tao Xu

Received: 13 October 2005 / Accepted: 23 January 2006 / Published online: 23 June 2006

Abstract The difference in time-resolved fluorescence spectrum between the cortical sarcoma and the adjacent normal tissue was studied in both experimental and theoretical ways. The Clinical data were obtained *in vivo* using a time-resolved fluorescence spectrometer employing a single fiber-optic probe for excitation and detection. Tissue was modeled as s-180 sarcoma tumor surrounded with normal muscle and was mediated by the Palladium-porphyrin photosensitizer (Pd-TCPP). The emitted fluorescence was considered as arising from the tumor tissue or the normal muscle, due to the presence of the photosensitizer. A computational code which could simulating time-resolved fluorescence emission was presented and applied to comparing fluorescence decay of photosensitizer in different stages of tumor growth. In this code the different stages of the tumor was modeled through changing the time τ, the delay of the fluorescence photon emission and $z_{\max}$, the thickness of the tumor. It was found in the *in vivo* experiment that the fluorescence from tumor tissue decayed more quickly than from the adjacent normal muscle. For the ten rats in the first experiment day, the mean decay constant of tumor T_s and normal tissue T_n were 554 and 526 μs, respectively. And T_s increased with the tumor growth, from 554 μs in the first day to 634 μs in the eighth day while T_s kept steady. It was believed that the more adequate oxygen supplied by the normal tissue can more effectively quench the fluorescence and in the normal tissue the photosensitizer lifetime is smaller. As a result the simulated time-resolved fluorescence spectrum of normal tissue showed more quickly decay. And the thickness of the tumor can also delay the fluorescence decay. Both the experimental and simulated results indicated that the germination of the tumor would increase the decay constant of the time-resolved fluorescence spectrum. So decay constant of the tumor tissue spectrum should be larger than that of adjacent normal tissue for the reason of hypoxia and overgrouth. This fact could be of use in the tumor diagnoses.

Keywords Time-resolved spectrum · Monte Carlo simulation · Fluorescence lifetime · Decay constant

Introduction

Fluorescence spectroscopy is an optical method that can provide rapid differentiation between tumor and normal tissue in a variety of epithelial organ systems. When tissue is illuminated with specific wavelengths light, fluorescent biological molecules will absorb the energy and emit it as fluorescent light at longer wavelengths. Furthermore, there are nonfluorescent light absorbers and scatterers in tissues that modulate the tissue fluorescence intensity at the excitation and emission wavelengths. Diffuse reflectance spectroscopy is another optical method that provides direct measurement of light absorption and scattering. The fluorophores can be either endogenous to the tissue or exogenous in the form of an injectable fluorescent molecule. The advantage of using exogenous fluorophores is that the photophysical and pharmacokinetic properties can be selected and are known. Furthermore, higher fluorescence intensity and longer fluorescence lifetime can be obtained than that from endogenous fluorophores. So much work has been done for the tumor diagnoses with the frequency-domain fluorescence spectrum

Y. Li
College of Engineering and Technology, Shenzhen University, Shenzhen, P.R. China

M. Li · T. Xu (✉)
Academy of Metrology and Quality Inspection of Shenzhen, Shenzhen, P.R. China
e-mail: xutao780606@126.com

in the fields of expanded skin [1, 2], lung [3], mammary gland [4], gastrointestinal tract [5], gullet [6], and brain [7], etc. While those fluorescence measurements are relatively simple to implement clinically and appear to provide useful diagnostic information, there are certain limitations intrinsic to the steady-state spectral technique. Limitations to spectrally resolved fluorescence measurements arise from the fact that these steady-state measurements integrate the emitted fluorescence signal over time, thus ignoring the dynamics of the fluorescence decay and losing an additional dimension of information. Fortunately, these limitations may be addressed by using time-resolved detection, which provides complementary information. Time-resolved techniques capture the transient decay of the fluorescence intensity in time, which reflects the fluorescence lifetime. The fluorescence lifetimes, which depend on both radiative and nonradiative decay mechanisms, are known to be extremely sensitive to the local biochemical environment [8]. Further, because spectrally resolved measurements are inherently intensity dependent, variations in intensity resulting from optical loss in the experimental system or optical absorption in complex media may affect the line shape of the steady-state emission spectrum in unpredictable and unquantifiable ways [8]. This is an important issue to consider when applying fluorescence spectroscopy *in vivo*, since intensity losses attributed to hemoglobin absorption in tissue are routinely observed *in vivo* [5, 9]. Because the fluorophore lifetime does not change with variations in excitation intensity or optical losses from hemoglobin absorption, time-resolved measurements are intensity independent [8]. Until recently, time-resolved fluorescence spectroscopy had been employed exclusively for *in vitro* diagnosis of tissue specimens and in this paper we used it to study the difference of the cortical sarcoma and the adjacent normal tissue.

In order to quantify changes between the fluorescence of normal and dysplastic pathologies for a variety of epithelial tissues, previous researchers have employed the use of Monte-Carlo simulations since the simulations provide an accurate method to model light transport in turbid media [10, 11]. In this manuscript, we employ a Monte-Carlo simulation to model time-resolved fluorescence collected *in vivo*. Before doing that we have described how the tumor tissue is modeled and discuss the effects of varying physical properties of the tissue to explain the observed difference in the *in vivo* experiment.

Materials and methods

Fluorophore preparation

Pd-*meso*-tetra(4-carboxyphenyl)porphyrin (Pd-TCPP) was purchased from Porphyrin Products Inc in US and was made 10 μM solution. The compound was dissolved in 0.5% bovine serum albumin (BSA) as a stock solution for administration to the animals.

Animal procedures

Ten Wistar rats weighted 200 $\pm$ 10 g (Experimental Animal Center of PLA General Hospital, Beijing, China) were obtained one week before the experimentation. They were housed in a room with subdued lighting and fed with a standard pellet diet and water. Sarcoma tumor cell suspension was transplanted into the right armpit of each mouse. The tumors that grew to approximately 6–7 mm in size within about 5 days after transplantation were used in this experiment. The animals were injected Pd-TCPP solution of 10 mg/mL directly into the tumor area at a dose of 2.5 mg kg^{-1}. About 3 hr later the rats were anaesthetized with 50 mg kg^{-1} sodium pentobarbital. The skins were slit and flooded with saline and the time-resolved spectroscopy of the tumor area and adjacent normal tissue were detected by a homemade instrument which would be introduced in the next paragraph. Then the skins were sutured and the rats were housed. The same procedures were performed per day in the following 7 days.

Experimental apparatus

The homemade instrument was based on exciting and detecting time-resolved fluorescence using a single optical fiber. A schematic of the apparatus is shown in Fig. 1. A frequency doubling semiconductor laser (Biomedical Engineering Department of Tianjin Medical university, Tianjin, China) was used as a 532 nm excitation source. This laser can export laser pulse with pulse width of 1 ms and pulse energy of 1 mJ. The output light was was coupled into a mirror assembly (ThorLabs, Newton, New Jersey) that separated fluorescence from the excitation light using a thin dichroic mirror (Oriel, Stratford, Connecticut). The mirror/lens assembly coupled the excitation light into a single 200 mm optical fiber probe, which was used to excite and detect the fluorescence. The fluorescence collected by the probe was reflected from the mirror into an optical fiber coupled to a photomultiplier tube (R2228, Hamamatsu, Japan). The fluorescence was filtered with 650 nm cut-on and 630–650 nm band-pass filters (Oriel, Stratford, Connecticut) to reduce the signal from scattered excitation light (from the mirror and the sample) and to limit the spectral width of the detected fluorescence. The pulse from the photomultiplier tube was amplified, time delayed, and used as a "start" input to a time-correlated single photon counting card (SPC-630, Becker&Hickl, Germany) operated in reversed "start-stop" mode. The "stop" input was from an electronic synchronization pulse from the laser driver.

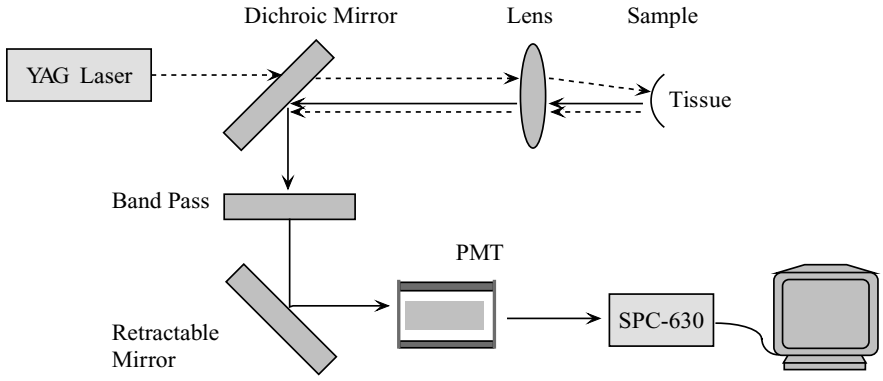

Fig. 1 Experimental apparatus for time-resolved spectrum measurements. The *dotted line* is the excitation path and the *solid gray line* the fluorescence. The single photon counting (TCSPC) module was run in reverse time mode, with the time measurement started by the detection of a photon

In vivo experiment

Fluorescence measurements were performed at tumor areas and the adjacent normal tissues on the right armpit of the rats. The dectect sites were shaved and then depilated with a hair removal product. Fluorescence decay was measured in the muscle (fiber embedded about 5 mm below the surface) using the single optical fiber. An 18-gauge needle was used to guide the fiber into the muscle, and was removed before commencing the fluorescence measurement. The background for the time-resolved system was the average of the signal measured with the fiber tip in water and in air. Time-resolved data were fitted to a single exponential decay:

$$I(t) = I(0)\, e^{-t/T} + B \tag{1}$$

where $I(t)$ is the fluorescence intensity at time t, and T is the decay constant of the time-resolved spectrum.

Time-resolved spectrum simulating

The traditional Monte Carlo algorithm developed by Wang etc. [12] was improved to take into account the structural characters and oxygen status of the tumor area. The weight array w_i was set according to the time series. The size of step s_i is converted into flight time in the tissue. The total time of every flight corresponded to one of the bins of time series. And the weight of the photon in this flight is recorded into the corresponding bin of the weight array when the flight direction $d_z < 0$ and the point coordinate $z < 0$. To simulate fluorescence emission, before each scattering event of an excitation photon, a random number (between 0 and 1), ζ_1, is generated and compared to a fluorophore absorption threshold value, κ, where $\kappa = \exp(-\mu_{af} s_i)$, and μ_{af} is the coefficient of fluorophore absorption. If ζ_1 is less than κ, the excitation photon is tagged a fluorescence photon. The final weight of the photon, which had been regarded as a fluorescence photon, was recorded in the bins of time series. The fluorophore lifetime, τ, is the average amount of time electrons spend in the excited state. Electrons that decay radiatively emit fluorescence photons that the simulation delays in time by a variable factor t_d, where t_d is given by $t_d = -\tau \ln(\zeta_2)$ and ζ_2 is a random number between 0 and 1. Time the photons spent in the tissue was composed of the flight time and the emitting decay time, t_d. The optical-transport coefficients and fluorophore's optical properties was list in Table 1, referring some former studies [13–15].

In this simulation, the different stages of the tumor was modeled through changing the time τ, the delay of the fluorescence photon emission and z_{max}, the thickness of the tumor. It was believed that the delay of the fluorescence photon emission of normal tissue is smaller than that of tumor because it could supply adequate oxygen which can effectively quench the fluorescence. As a result the simulated time-resolved fluorescence spectrum of normal tissue showed more quickly decay. In the *in vivo* experiment we can not measure the tumor thickness and think empirically that the tumor thickness increase with the tumor growth.

Results

The time-resolved fluorescence spectrum for representative normal (dashed line) and tumor tissue (solid line) detected in the first day by the homemade instrument are shown in Fig. 2. As is discernible by eye, the normal decay is faster compared to the sarcoma tissue. Analyzing the fluorescence decay traces shown in the Fig. 2 using Eq. (1), the decay constant of the normal tissue and the sarcoma tissue is 529 μs and 564 μs. Decay constant of all the ten rats are obtained by this way and the mean decay constant, T_s and T_n, in the first day are 554 μs and 526 μs respectively. It can be concluded statistically that the decay constant of sarcma tissue is obviously larger than that of adjacent normal tissue ($p = 0.026$). The mean decay constants in the eight days are record in Fig. 3. For two rats die in the seventh day and one rat dies in the eighth day, the datas in those two days are the mean values of 8 and 7 dates respectively. The tumor growth seems to enlarge T_s while has little influence on T_s. Starting at a mean decay constant of 554 μs, T_s changes to

Table 1 Values of Some Optic Parameters in the Simulation Program.

Scatter coefficient	Absorption coefficient	Anisotropy factor	Fluorescence absorption coefficient	Normal tissue refractive index	Tumor refractive index
240 cm^{-1}	1.0 cm^{-1}	0.8	2.0 cm^{-1}	1.37	1.48

be 634 μs after 7 days of tumor growth. While T_n changes little and there is not obviouse difference between the first and the eighth day.

Figure 4A shows the simulated time-resolved fluorescence with varying tumor thickness and the same photosensitizer lifetime. The tumor thickness is varied as $z_{max} = 1$ mm, $z_{max} = 2$ mm and $z_{max} = 4$ mm and the photosensitizer lifetime is fixed at $\tau = 550$ μs. The simulated T_s are 535 μs, 582 μs, and 604 μs respectively. Figure 4B shows the time-resolved fluorescence with varying photosentitizer lifetime and the fixed tumor thickness. The lifetime is varied as $\tau = 550$ μs, $\tau = 600$ μs and $\tau = 650$ μs and the tumor thickness is fixed at $z_{max} = 2$ mm. The simulated T_s are 582 μs, 643 μs, and 691 μs respectively. The increase of both the tumor size and the photosensitizer lifetime can increase the decay constant of the time-resolved fluorescence spectrum.

Discussion

The search coverage in the experiment is the sarcoma tissue at the right armpit of rats and the adjacent normal tissue. We find that the time-resolved fluorescence spectrum of sarcoma tissue decays more slowly than that of the adjacent normal tissue. We explore the mechanism through an improved Monte Carlo simulation that consider the intensity decay against time. It is concluded that the spectrum decay constant is affected by the delay of the fluorescence photon emission (the fluorophore lifetime) and the tumor thickness. It is mentioned in some previoous studies that thick turbid medium can delay the escape of flight photons by increasing the flight path and collision probability [16–18]. This is consistent with the simulating result showed in Fig. 4A. As it is not difficult to be aware that the tumor thickness increasing with the tumor growing, we can think it well-founded that tumor thickness is one of the impact factors that lead to the experimental result showed in Fig. 3.

From Fig. 4B, it can be conclude that the lifetime of the fluorophore can also delay the fluorescence photons emission. It is indicated in some studies the fluorophore lifetime is strongly depend on the surround oxygen environment [19–22]. The oxygen dependence of the fluorophore lifetime can be described by the Stern–Volmer relationship:

$$\frac{\tau_0}{\tau} = 1 + k_q \cdot \tau_0 \cdot [O_2] \tag{2}$$

where τ_0 is the fluorophore lifetime in the absence of oxygen and is decided by the characters of photosensitizer, k_q is the fluorescence quenching constant. As the oxygen content of tumor tissue is lower than that of the adjacent normal tissue [23], the lifetime of fluorophore in tumor is longer than that in normal tissue according to Eq. (2). As a result the decay constant of time-resolved fluorescency spectrum is higher in tumor than in the adjacent normal tissue. This can explain the experimental result showed in Fig. 2. Furthermore, the tumor oxygen decreases with the tumor growing [24, 25]. According to the logic described above, the decay constant

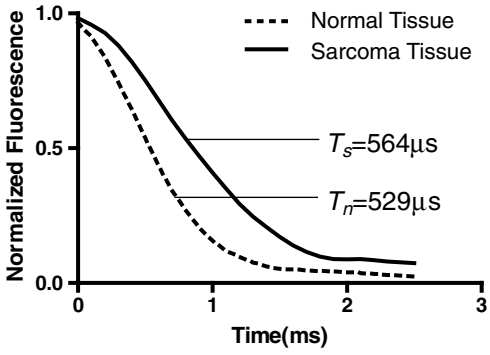

Fig. 2 Representative time-resolved fluorescence spectrum of the sarcoma tissue and the adjacent normal tissue detected in the *in vivo* experiment. The value T_s and T_n are obtained by fitting the datas to Eq. (1)

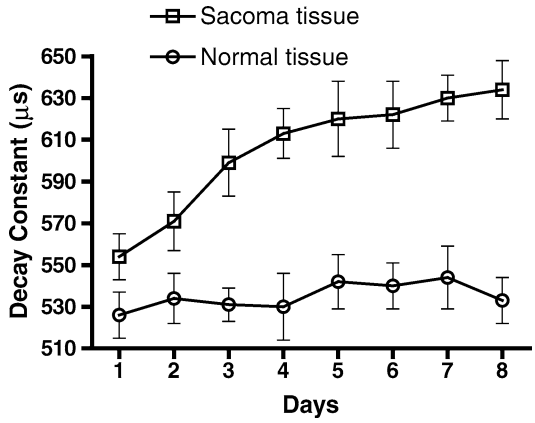

Fig. 3 Changes of the decay constant with the growth of tumor. Datas in 1–6 days are obtain from 10 experimental rats. The datas in the other 2 days are the mean values of eight and seven rats, respectively. For the normal tissue, it is proved by a Wilcoxon signed rank test that there is no obvious difference in T_s between the first days (with minimum mean $T_s = 526$ μs) and the seventh day (with the maximum mean $T_s = 544$ μs)

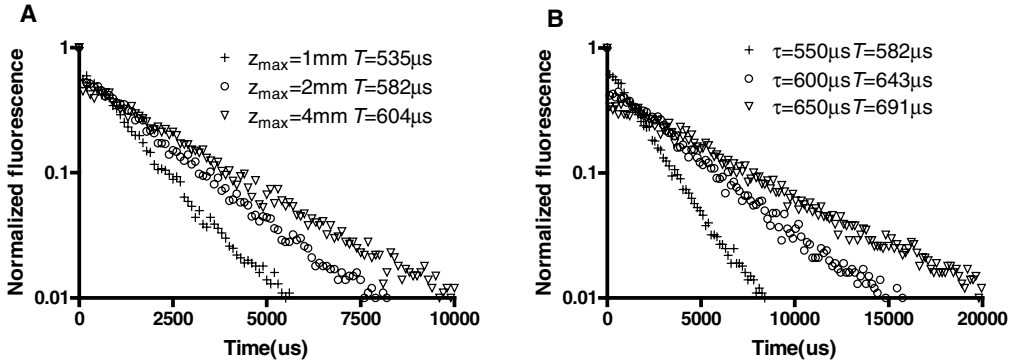

Fig. 4 Simulated time-resolved fluorescence decays for varying tumor thickness (**A**) and photosensitizer lifetime (**B**). Each simulation get all parameters from Table I and the result T is calculated by fitting each simulated trace to Eq. (1)

of time-resolved fluorescency spectrum increases with the tumor growth.

The exogenous fluorophores need to be of long lifetime to distinguish the spectrum difference between the normal and tumor tissue. Verteporfin (QLT Inc, Vancouver, Canada) with a lifetime of 6 ns and pyrene butyric acid with a lifetime of 500 ns are used as photosensitizer in our *in vivo* experiment. While we can not find well-regulated difference in time-resolved fluorescence spectrum between the normal and tumor tissue in that tries. For short lifetime photosensitizer, the time that electrons stay on the excited state is comparative with the time that photons fly in the medium. Thus in thousands of flight defined in one time of the Monte Carlo simulation the time from the entrance of exciting photon to overflow of the fluorescence photon distributes randomly and we can not obtain consilient fluorescence spectrum in several times of simulation. Despite the use of precise instrument the correct spectrum can not be detected for the short lifetime of photosensitizer. And the spectrum difference between the normal and tumor tissue can not be observed as a result.

References

1. Zeng H, MacAulay C, Palcic B Mclean DI (1993) A computerized autofloruescence and diffuse reflectance spectroanalyser for in vivo skin studies. Phys Med Biol 38:231–240
2. Zeng H, MacAulay C, McLean DI, Palcic B (1993) Novel microspectrophotometer and its biomedical applications. Opt Eng 32(8):1809–1813
3. Alfano RR, Tang GC, Pradhan A, Lam W (1987) Fluorescence spectra from cancerous and normal human breast and lung tissues. IEEE J Quantum Electron QE-23:1806–1811
4. Ramanujam N, Mitchell MF, Mahadevan A, Thomsen S, Malpica A, Wright T, Atkinson A, Richards-Kortum RR (1996) Development of a multivariate statistical algorithm to analyze human cervical tissue fluorescence spectra acquired in vivo. Lasers Surg Med 19(1):46–62
5. Schomacker KT, Frisoli JK, Compton CC, Flotte TJ, Richter JM, Nishioka NS, Deutsch TF (1992) Ultraviolet laser-induced fluorescence of colonic tissue: basic biology and diagnostic potential. Lasers Surg Med 12:63–78
6. Panjehpour M, Overholt BF, Schmidhammer JL, Farris C, Buckley PF, Vo-Dinh T (1995) Spectroscopic diagnosis of esophageal cancer; new classification model, improved measurement system. Gastrointest Endosc 45:577–581
7. Bottiroli G, Croce AC, Locatelli D, Nano R, Giombelli E, Messina A, Benericetti E (1998) Brain tissue autofluorescence: An aid for intraoperative delineation of tumor resection margins. Cancer Detect Prev 22(4):330–339
8. Lakowicz J (1983) Principles of fluorescence spectroscopy. Plenum, New York
9. Schomacker KT, Frisoli K, Compton CC, Flotte TJ, Richter JM, Deutsch TF (1992) Ultraviolet laser-induced fluorescence of colonic polyps. Gastroenterology 102:1155–1160
10. Zonios G, Cothren R, Arendt J, Wu J, Van Dam J, Crawford J, Manoharan R, Feld M (1996).Morphological model of human colon tissue fluorescence. IEEE Trans Biomed Eng 43:113–122
11. Drezek R, Sokolov K, Utzinger U, Boiko I, Malpica A, Follen M, Richards-Kortum R (2001) Understanding contributions of NADH and collagen to cervical tissue fluorescence spectra: Modeling, measurements, and implications. J Biomed Opt 6:385–396
12. Wang LH, Steven LJ, Zheng LQ (1995) MCML-Monte Carlo modeling of light transport in multi-layered tissues. Comput Methods Programs Biomed 47:131–146
13. Mycek MA, Vishwanath K, Pogue BW, Schomacker KT, Sishioka NS (2003) Simulation of time- resolved fluorescence in multi-layered biological tissues: applications to clinical data modeling. Proc SPIE 4958:51–59
14. Cheong WF, Prahl SA, Welch AJ (1990) A review of the optical properties of biological tissues. IEEE J Quantum Electron 26:2166–2185
15. Bolin FP, Preuss LE, Taylor RC (1989) Refractive index of some mammalian tissues using a fiber optic cladding method. Appl Opt 28(12):2297–2304
16. Rebecca RK, Eva SM (1996) Quantitative optical spectroscopy for tissue diagnosis. Annu Rev Phys Chem 47:555–606
17. Wang LH, Jacques SL, Zheng LQ (1995) MCML-Monte Carlo modeling of light transport in multi-layered tissue. Comput Methods Programs Biomed 47:131–146
18. Ramanujam N (2000) Fluorescence spectroscopy in vivo. Wiley, Chichester, UK
19. Zheng L, Golub AS, Pittman RN (1996) Determination of PO_2 and its heterogeneity in single capillaries. Am J Physiol 271(Heart Circ Physiol) 40:H365–H372
20. Sinaasappel M, Ince C (1996) Calibration of Pd-porphyrin phosphorescence for oxygen concentration measurements in vivo. J Appl Physiol 81(5):2297–2303

21. Torres Filho IP, Intaglietta M (1993) Microvessel PO2 measurements by phosphorescence decay method. Am J Physiol 265(Heart Circ Physiol) 34:H1434–H1438
22. Wilson DF, Rumsey WL, Green TJ, Vanderkooi JM (1987) The oxyen dependence of mitochondrial oxidative phosphorylation measured by a new optical method for measuring oxygen concertration. J Biol Chem 25:2712–2718
23. Braun RD, Lanzen JL, Snyder SA, Dewhirst MW (2001) Comparison of tumor and normal tissue oxygen tension measurements using OxyLite or microelectrodes in rodents. Am J Phusiol (Heart Circ Physiol) 280:H2533–H2544
24. Dewhirst MW, Ong ET, Klitzman B, Secomb TW, Vinuya RZ, Dodge R, Brizel D, Gross JF (1992) Perivascular oxygen tensions in a transplantable mammary tumor growing in a dorsal flap window chamber. Radiat Res 130:171–182
25. Dewhirst MW, Ong ET, Braun RD, Smith B, Klitzman B, Evans SM, Wilson D (1999) Quantification of longitudinal tissue PO2 Gradients in widow chamber tumours: impact of tumour hypoxia. Br J Cancer 79:1717–1722